On the chaotic nature of solar-terrestrial environment: Interplanetary Alfvén intermittency

A. C.-L. Chian,[1,2] Y. Kamide,[2] E. L. Rempel,[3] and W. M. Santana[1]

Received 31 August 2005; revised 28 April 2006; accepted 3 May 2006; published 7 July 2006.

[1] We present an overview of observational and theoretical evidence of chaos and intermittency in the solar-terrestrial environment including solar dynamo, solar atmosphere, solar wind, and terrestrial magnetosphere-ionosphere-atmosphere. The chaotic nature of space plasmas is studied by a nonlinear model of Alfvén waves described by the low-dimensional limit of the derivative nonlinear Schrödinger equation given by its stationary solutions in the frame moving with the driver wave velocity. A periodic window of the bifurcation diagram is constructed to identify two types of Alfvén chaos related to type-I intermittency and crisis-induced intermittency. We show that an Alfvén chaotic attractor is composed of chaotic saddles and unstable periodic orbits and explain the links between these unstable structures and Alfvén intermittency. The role of interplanetary Alfvén intermittency in the solar wind driving of intense geomagnetic activities is discussed.

Citation: Chian, A. C.-L., Y. Kamide, E. L. Rempel, and W. M. Santana (2006), On the chaotic nature of solar-terrestrial environment: Interplanetary Alfvén intermittency, *J. Geophys. Res.*, *111*, A07S03, doi:10.1029/2005JA011396.

1. Introduction

[2] Sun-Earth system is a complex, electrodynamically coupled system dominated by nonlinear interactions. The complex behaviors of the solar-terrestrial system, e.g., the phenomena of solar flares and magnetospheric substorms, are an indication that it is in a state far from equilibrium whereby instabilities, nonlinear waves, and turbulence play key roles in the system dynamics. One of the ubiquitous features of the complex space environment is the occurrence of intermittency and chaos in solar dynamo, solar corona, solar wind, and Earth's magnetosphere-ionosphere-atmosphere. Intermittency is characterized by abrupt changes of the physical variables in space and/or time, e.g., the variation of the amplitude or phase of the solar wind magnetic field, with alternating periods of quiescent low-level fluctuations and bursting high-level fluctuations; it displays multiscale behaviors with power-law spectrum in frequency and wave number, as well as non-Gaussian statistics in the probability distribution function of fluctuations. Chaos is characterized by aperiodic fluctuations in space and/or time, which are sensitive to small changes in the initial conditions and system parameters. We present first an overview of previous results related to the observational and theoretical evidence of intermittency and chaos in the solar-terrestrial environment.

[3] Solar activity, including the dynamics and structure of the solar atmosphere, is controlled by the magnetic fields generated by the combined action of convection and differential rotation of a nonlinear dynamo in the solar interior [see, e.g., *Weiss and Tobias*, 2000; *Gómez et al.*, 2004]. The observed time series of sunspot cycles is intermittent, showing periods of large-amplitude cyclic fluctuations which are irregularly interrupted by quiescent periods of reduced magnetic activity, called the grand minima, such as the Maunder Minimum and the Spoerer Minimum [*Kremliosvsky*, 1995; *Moussas et al.*, 2005]. Simulations of a mean-field model of solar dynamo show many features seen in the solar cycle, such as quasi-periodicity, intermittency, and long periods of low activity [*Hoyng*, 1993]. *Kurths et al.* [1993] found chaos in numerical simulations of both three-dimensional (3-D) MHD and simplified low-dimensional mean field models of nonlinear dynamo. A simple third-order model of solar dynamo suggests that modulation of the solar cycle is chaotic, described by a bifurcation diagram, which can explain the recurrent features of grand minima [*Tobias et al.*, 1995]. *Ossendrijver and Covas* [2003] reported the evidence of crisis-induced intermittency due to attractor-widening in a 2-D solar dynamo model driven by the buoyancy instability of magnetic flux tubes and showed that the average duration of the grand minima follows a theoretically predicted scaling. *Charbonneau et al.* [2004] showed that a solar cycle model based on the Babcock-Leighton mechanism of poloidal field regeneration can exhibit intermittency in the presence of low-amplitude noise. Numerical simulations of the solar

[1]National Institute for Space Research (INPE) and World Institute for Space Environment Research (WISER), São José dos Campos, São Paulo, Brazil.
[2]Nagoya University, Solar-Terrestrial Environment Laboratory, Toyokawa, Japan.
[3]Institute of Aeronautical Technology (ITA) and World Institute for Space Environment Research (WISER), São José dos Campos, São Paulo, Brazil.

0148-0227/06/2005JA011396

magnetic activity cycle show a well-defined transition to chaos via period-doubling bifurcations [*Charbonneau et al.*, 2005].

[4] In a 2-D simulation of MHD turbulence of solar active regions, *Dmitruk et al.* [1998] showed that the energy dissipation rate as a function of time of a coronal loop displays the relaxation of the system to a stationary regime with intermittent behavior, in the form of impulsive events of magnetic energy dissipation associated with nanoflares. The highly intermittent nature of dissipation in MHD turbulence is revealed in a numerical simulation of coronal loop subject to random magnetic forcing, with clear indication of intermittency in both space and time even for moderate magnetic Reynolds numbers [*Georgoulis et al.*, 1998]. *Boffetta et al.* [1999] suggested that the power-law statistics of the quiet time interval between successive bursts of solar flares is an indication of an underlying complex dynamics with long correlation times; a chaotic shell model of intermittent MHD turbulence was able to reproduce the observed power-law statistics. Evidence of intermittency in the transition region was recorded in a quiet Sun by SOHO/SUMER [*Patourakos and Vial*, 2002]; these findings render support for an impulsively heated transition region and corona via intermittent MHD turbulence. Resonant heating of ions in the solar corona by large-amplitude Alfvén waves and electrostatic waves propagating across the magnetic field was studied by *White et al.* [2002], which demonstrates the existence of the resonances leading to chaos and significant heating. *Markovskii and Hollweg* [2004] developed a model of intermittent heating of solar corona by ion cyclotron waves produced by small-scale reconnection events related to microflares; their calculations suggest that the overall heating is sufficiently efficient to account for the acceleration of the fast solar wind in solar coronal holes. A model of coronal nanoflares was formulated by a shell technique based on a set of reduced MHD equations [*Veltri et al.* [2005]; numerical simulations show that the injected energy is efficiently stored in the coronal loop where a significant level of magnetic and velocity fluctuations is obtained, leading to nonlinear interactions that give rise to an energy cascade toward small scales where energy is intermittently dissipated.

[5] The first observation of nonlinear evolution from order to chaos of solar wind was reported by *Burlaga* [1988], who identified the formation of ordered large structures from irregular small structures as well as the period-doubling of the period of the corotating interaction regions in the outer heliosphere. *Burlaga* [1991] was also the first to report the evidence of intermittent turbulence in the solar wind, by demonstrating the existence of multifractal structure in the velocity fluctuations associated with recurrent streams at 1 AU and near 6 AU. *Marsch and Liu* [1993] provided evidence of the intermittent nature of the fluctuations of the flow velocity and Alfvén velocity in the inner heliosphere between 0.3 and 1.0 AU. *Marsch and Tu* [1994] determined the non-Gaussian nature of the probability distribution functions of the interplanetary intermittent turbulence, by showing that at small scales the statistical properties are dominated by large-amplitude fluctuations. *Chian et al.* [1998] and *Borotto et al.* [2001] demonstrated that the interplanetary Alfvén intermittency can be driven by chaos. *Matthaeus et al.* [1999] formulated a phenomenological theory for the radial evolution of MHD and Alfvénic turbulence in the solar wind which includes a simple closure for local anisotropy, spatial transport, and driving by large-scale shear and pickup ions. *Sorriso-Valvo et al.* [1999] showed that the non-Gaussian behavior of the probability distribution functions of solar wind velocity and magnetic field fluctuations at small scales are represented by a convolution of Gaussians whose variances are distributed according to a log-normal distribution; their results confirm the findings of *Marsch and Tu* [1994] that in both fast and slow solar winds, the magnetic field is more intermittent than the bulk speed. *Bruno et al.* [2001] applied the wavelet technique to determine the local intermittency measure in the solar wind data and identify the intermittent structures contributing to a single event of solar wind intermittency; their results show that this event is located at the border between two adjacent interplanetary regions characterized by different total pressure and bulk velocity, possibly the boundary between two adjacent flux tubes; these observations render support for the idea that the solar wind fluctuations are a superposition of propagating Alfvén waves and flux tubes of convected-pressure-balance structures originated at the base of the solar atmosphere. *Gulamali and Cargill* [2001] discussed the character of MHD turbulence in the well-developed corotating interaction regions at midlatitudes of the heliosphere based on the Ulysses data; their magnetic field power spectra show evidence for the turbulent mixing of plasma far from the Sun and the possible signs of instabilities arising at stream interfaces; there is a clear variation of magnetic field power and Alfvenicity with the structure of the corotating interaction regions; in addition, they found that the solar cycle variation has a clear effect upon the turbulent character of the solar wind thus provides further evidence for the solar origin of the majority of interplanetary turbulence. *Padhye et al.* [2001] used the Ulysses observations to examine the probability distribution functions of the fluctuations of the fast and slow solar wind magnetic field at different phases in the solar cycle and determine the degrees of non-Gaussianity of the interplanetary intermittent turbulence by moment comparisons (kurtosis). *Pagel and Balogh* [2003] studied the radial dependence of intermittency in the fast polar solar wind magnetic field using the Ulysses data. *Bruno et al.* [2004] compared observations of interplanetary fluctuations with a Levy statistics and showed that the observations can be reasonably fitted by a truncated-Levy-flight distribution; they proposed a two-component model for the solar wind intermittent turbulence, one represented by coherent, nonpropagating structures convected by the solar wind and the other composed of propagating, quasi-stochastic fluctuations, namely Alfvén waves. *Burlaga and Viñas* [2004] described the multiscale structure of fluctuations in the solar wind speed and magnetic field strength at 1 AU by a generalized Tsallis probability distribution function from a nonadditive entropy function in the context of nonextensive statistical mechanics; many types of physical structures were identified, including intermittent turbulence at small scales. *Bruno and Carbone* [2005] and *Bruno et al.* [2005] reviewed theories and observations of MHD intermittent turbulence in the solar wind. *Hnat et al.* [2005] used extended self-similarity to reveal scaling in the structure functions of

density fluctuations in the solar wind. *Leubner and Vörös* [2005] adopted a nonextensive entropy approach to analyze the scale dependence of the solar wind intermittency and showed that the observed Wind and ACE probability distribution functions are accurately reproduced by the theoretical bi-kappa distributions for different scales.

[6] The auroral electroject (AE) index is commonly used as an indicator of the global magnetospheric activity, with a viewpoint that AE can sample the state space of the magnetospheric system. *Price and Prichard* [1993] considered the nonlinear response of the magnetosphere to the solar wind forcing, as given by the AE index, for 30 October 1978 when the interplanetary magnetic field has a nearly constant southward value of $B_z = -10$ nT and the auroral activity was quite high; they found that there is some evidence for deterministic nonlinear response of the magnetosphere to solar wind forcing. *Pu and Wang* [1997] studied the structure instability and nonlinear evolution of magnetic islands produced by magnetic reconnection at the magnetopause and derived the critical conditions for occurrence of bifurcation and chaos. *Consolini and De Michelis* [1998] calculated the probability distribution functions of the AE-index fluctuations at different timescales from 1 January 1978 to 31 December 1985, which indicates that the distributions are always non-Gaussian for the timescales in the range 1–120 min for both quiet and disturbed geomagnetic periods, which indicates that the auroral electrojet is intermittent for both periods. *Angelopoulos et al.* [1999] obtained evidence of intermittent turbulence in the Earth's plasma sheet using the Geotail and Wind data, which permits cross-scale coupling of localized jets (bursty bulk flows) into a global perturbation (substorms) with demonstrated characteristics of self-organized criticality; according to their observations the magnetotail is in a bimodal state: nearly stagnant, except when driven turbulent by bursty fast flows; they pointed out that processes other than self-organized criticality, such as chaos, can also be associated with intermittency. *Kovács et al.* [2001] performed discrete orthonormal wavelet transform and filtering in the midlatitude geomagnetic time series in order to identify the intermittent events characterized by non-Gaussian probability distribution functions; they computed the empirical probability distributions of the laminar time between the energy bursts of intermittent events and argued that near-SOC or chaotic turbulence model can explain the observed features. *Choe et al.* [2002] found characteristics of self-similarity and self-organized criticality of the AL time series, and a good correlation between AL and the solar cycle. *Consolini and De Michelis* [2002] studied the fractal statistics of the AE-index burst waiting times between quiet and active periods of auroral activities, which supports the hypothesis that the Earth's magnetotail might operate as a complex system near a marginally stable state and plays a relevant role in the impulsive energy relaxation. *Chang et al.* [2003] described a complexity theory for forced and/or self-organized criticality for space plasmas far from equilibrium and showed that the sporadic and localized interactions of magnetic coherent structures are the origin of intermittent turbulence and complexity in space plasmas. *Hnat et al.* [2003] studied scaling in data sets of the geomagnetic indices (AE, AU, and AL) and the ε parameter which is a measure of the solar wind driver as seen by the Wind spacecraft. *Stepanova et al.* [2003] found that the probability distribution functions of the Polar Cap index display a strong non-Gaussian shape, indicating intermittency of magnetospheric dynamics. *Chang et al.* [2004] used the probability distribution function and local intermittency measure to characterize the sporadic, localized, and scale-dependent nature of intermittent turbulence using the results of 2-D MHD simulations. *Vörös et al.* [2004] investigated small-scale intermittent magnetic turbulence observed by Cluster in the plasma sheet using a wavelet estimator; they showed that during nonbursty bulk flow associated periods the energy transfer to small scales is absent, whereas cross-scale energy transfer is seen during bursty bulk flow associated periods. *Zelenyi and Milovanov* [2004] reviewed the modern theory of turbulence in complex dynamical systems displaying self-organized critical behavior and power-law energy spectra and discussed its application to current sheet, substorm, and large-scale magnetic fields in solar photosphere and interplanetary space. *Consolini and De Michelis* [2005] applied the technique of local intermittency measure to obtain evidence of the two-component model of auroral electroject proposed by *Kamide and Kokubun* [1996] which consists of contributions from the directly driven convection enhancement and the impulsively unloading processes in the solar wind-magnetosphere interactions; by separating the two components of the AE index into a nonintermittent AE component related to the directly driven contribution and an intermittent AE component due to the unloading contribution, for the 30 October 1978 event previously considered by *Price and Prichard* [1993], they showed that the intermittent auroral events appear as coherent structures localized in time with timescales shorter than about 100 min, in agreement with the possible origin of unloading phenomena suggested by *Kamide and Kokubun* [1996]. *Weygand et al.* [2005] obtained evidence of intermittent turbulence in plasma sheet by studying the scaling behavior of the probability distribution functions and the multifractal structure function, based on the magnetic field data of Cluster II.

[7] The above discussions demonstrate clearly that the study of intermittency and chaos is essential for our understanding of the complex physical processes underlying the Sun-Earth relation. The aim of this paper is to apply the low-dimensional chaotic approach to probe the intermittent nature of the solar-terrestrial environment, based on the numerical simulation of a nonlinear model of stationary solutions (i.e., solutions are stationary in time) of Alfvén waves. Following the works of *Chian et al.* [1998] and *Borotto et al.* [2001], two types of Alfvén intermittencies are studied: type-I intermittency and crisis-induced intermittency. In contrast to the papers by *Chian et al.* [1998] and *Borotto et al.* [2001] wherein the dynamical role of the driver amplitude on nonlinear Alfvén waves was studied, in this paper we investigate the dynamical role of the plasma dissipation on nonlinear Alfvén waves. In particular, we show that unstable periodic orbits and chaotic saddles are the fundamental unstable structures responsible for intermittency/chaos in a nonlinear model of Alfvén waves. Our model indicates that nonlinear Alfvénic fluctuations might evolve towards phases of strong intermittency alternating with phases of laminar behavior. In addition, we show that the average duration of the laminar phases for both types of

Alfvén intermittency follows a theoretically predicted scaling, which can be relevant for space weather forecasting. The role of interplanetary Alfvén intermittency in the geomagnetic events driven by the solar wind, known as the High-Intensity Long-Duration Continuous Auroral Activity (HILDCAA), will be discussed.

2. Nonlinear Model of Alfvén Waves

[8] Nonlinear spatiotemporal evolution of Alfvén waves can be modeled by the derivative nonlinear Schrödinger equation (DNLS) [*Hada et al.*, 1990; *Chian et al.*, 1998]

$$\partial_t b + \alpha \partial_x \left(|b|^2 b \right) - i(\mu + i\eta)\partial_x^2 b = S(b, x, t), \tag{1}$$

where the wave is propagating along an ambient magnetic field B_0 in the x-direction, $b = b_y + ib_z$ is the complex transverse wave magnetic field normalized to the constant ambient magnetic field, η is the dissipative scale length, time t is normalized to the inverse of the ion cyclotron frequency $\omega_{ci} = eB_0/m_i$, space x is normalized to c_A/ω_{ci}, $c_A = B_0/(\mu_0\rho_0)^{1/2}$ is the Alfvén velocity, $\alpha = 1/[4(1-\beta)]$, $\beta = c_S^2/c_A^2$, $c_S = (\gamma P_0/\rho_0)^{1/2}$ is the acoustic velocity, and μ is the dispersive parameter. The external forcing $S(b, x,t) = Aexp(ik\phi)$ is a monochromatic left-hand circularly polarized wave with a wave phase $\phi = x - Vt$, where V is a constant wave velocity, A is the driver amplitude, and k is the driver wave number.

[9] In this paper we investigate the special solutions of equation (1) which are stationary in time with $b = b(\phi)$, whose first integral reduces to a coupled set of three ordinary differencial equations describing the transverse wave magnetic fields and the wave phase of nonlinear Alfvén waves

$$\dot{b}_y - \nu \dot{b}_z = \frac{\partial H}{\partial b_z} + a\cos\theta, \tag{2}$$

$$\dot{b}_z + \nu \dot{b}_y = -\frac{\partial H}{\partial b_y} + a\sin\theta, \tag{3}$$

$$\dot{\theta} = \Omega, \tag{4}$$

where $H = (\mathbf{b}^2 - 1)^2/4 - (\lambda/2)(\mathbf{b} - \hat{\mathbf{y}})^2$, the overdot denotes derivative with respect to the wave phase $\tau = \alpha b_0^2 \phi/\mu$ (henceforth called the time variable), the normalized dissipation parameter $\nu = \eta/\mu$, $b \rightarrow b/b_0$ (where b_0 is an integration constant), $\mathbf{b} = (b_y, b_z)$, $\theta = \Omega\phi$, $\Omega = \mu k/\alpha b_0^2$, $a = A/\alpha b_0^2 k$, $\lambda = -1 + V/\alpha b_0^2$. We assume $\beta < 1$, hence $\alpha > 0$.

[10] The set of equations (2)–(4) represent a forced oscillator with two control parameters, the driver amplitude a and the dissipative coefficient ν. In this paper, we will study the dynamical properties of Alfvén waves by varying ν. This parameter is defined as a phenomenological damping parameter denoting the damping of Alfvén waves due to wave-particle interactions such as cyclotron damping or Landau damping [*Ghosh and Papadopoulos*, 1987].

3. Alfvén Chaos

[11] A low-dimensional model of Alfvén chaos was formulated by *Hada et al.* [1990] based on the numerical solutions of equations (2)–(4); for the nondissipative (Hamiltonian) case, the solutions near the phase-space separatrices (soliton) in the Poincaré map become chaotic as the driver amplitude increases; for the dissipative case, the system displays routes to chaos via period-doubling bifurcation and tangent bifurcation. A series of works were published following the pioneer model of *Hada et al.* [1990]. *Buti* [1992] showed that nonlinear Alfvén waves in a multispecies plasma can be chaotic if the driver amplitude exceeds a certain threshold; heavier ions, such as helium in the solar wind and oxygen in comets, tend to reduce chaos. *Buti* [1997] demonstrated that even a small fraction of charged dust grains can suppress chaos in Alfvén systems which are chaotic in the absence of dust particles. *Chian et al.* [1998] and *Borotto et al.* [2001] identified two types of Alfvén intermittency driven by chaos. *Chian et al.* [2002a] reported a transition mechanism to Alfvén chaos via a boundary crisis whereby a chaotic attractor suddenly appears/disappears; the same period-9 unstable periodic orbit is responsible for mediating two successive boundary crises. *Borotto et al.* [2004a] studied an Alfvén interior crisis associated with an abrupt increase/decrease of the size of the chaotic attractor. *Borotto et al.* [2004b] demonstrated that in the period-3 periodic window studied by *Chian et al.* [1998] and *Borotto et al.* [2001] the same period-9 unstable periodic orbit is responsible for mediating a boundary crisis followed by an interior crisis. *Rempel and Chian* [2004] and *Rempel et al.* [2004a] examined the role played by nonattracting chaotic sets known as chaotic saddles, responsible for chaotic transients in Alfvén chaos, and showed that at the onset of chaos via a saddle-node bifurcation and at a chaotic transition via an interior crisis the gaps in the chaotic saddles are filled by coupling unstable periodic orbits.

[12] A high-dimensional analysis of Alfvén spatiotemporal chaos based on DNLS was conducted by *Ghosh and Papadopoulos* [1987], which indicates the transition of MHD oscillations from a coherent state to turbulence. A numerical study of acceleration of Alfvén solitons by *Nocera and Buti* [1996] based on DNLS shows that under the action of an external harmonic driver nonlinear wave interactions develop and evolve to spatiotemporal chaos. *De Oliveira et al.* [1997] studied Alfvén spatiotemporal chaos in a dispersive modulational regime by solving a set of coupled wave equations. *Buti* [1999] discussed spatiotemporal chaos in nonlinear Alfvén waves described by DNLS. *Buti et al.* [1999] studied the spatiotemporal evolution of nonlinear Alfvén waves in streaming inhomogeneous plasmas governed by a modified DNLS. *Krishan and Nocera* [2003] used DNLS to study the relaxation of an Alfvén turbulence evolved from four-wave interactions and inverse energy cascade to a state with soliton type structures. A series of papers have treated the high-dimensional wave phase dynamics of nonlinear Alfvén waves based on the Kuramoto-Sivashinsky equation [*Chian et al.*, 2002a; *Rempel and Chian*, 2003; *Rempel et al.*, 2004b; *Rempel et al.*, 2004c; *Rempel and Chian*, 2005].

[13] In this paper, we study the roles played by unstable periodic orbits and chaotic saddles in Alfvén type-I intermittency and Alfvén crisis-induced intermittency, based on the low-dimensional model of Alfvén chaos described by equations (2), (3)–(4). A bifurcation diagram, which pro-

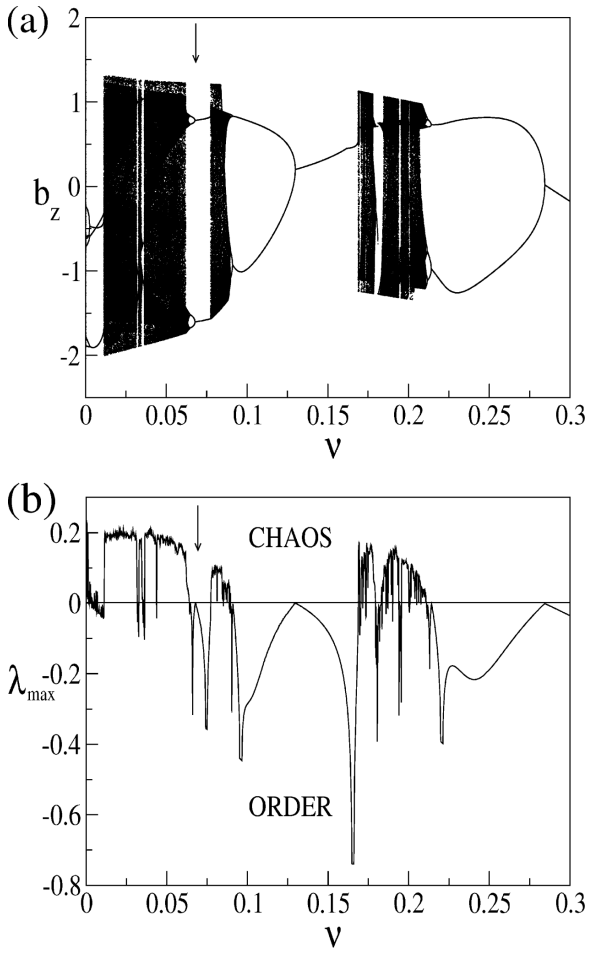

Figure 1. Bifurcation diagram and maximum Lyapunov exponent: global view. (a) Bifurcation diagram, b_z as a function of ν, (b) maximum Lyapunov exponent λ_{max} as a function of ν. Positive λ_{max} indicates chaos and negative λ_{max} indicates order. The arrow indicates a period-2 periodic window. $a = 0.3$, $\Omega = -1$, $\lambda = 1/4$, $\mu = 1/2$.

vides an overview of the system dynamics and its sensitive dependence on small variations in a system parameter, can be constructed from the numerical solutions of equations (2), (3)–(4) by varying the dissipative parameter ν while keeping other system parameters fixed ($a = 0.3$, $\Omega = -1$, $\lambda = 1/4$, $\mu = 1/2$). We define a Poincaré plane as

$$P : \left[b_y(\tau), b_z(\tau)\right] \rightarrow \left[b_y(\tau + T), b_z(\tau + T)\right], \qquad (5)$$

where $T = 2\pi/\Omega$ is the driver period. Figure 1a displays a global view of the bifurcation diagram of nonlinear Alfvén waves. For a given ν, Figure 1a plots the asymptotic values of the Poincaré points of b_z, where the initial transient is omitted.

[14] The phase space of equations (2)–(4) has three dimensions, therefore the system has three Lyapunov exponents, one of which is always zero (in the direction tangent to flow). For the remaining two exponents, the maximum Lyapunov exponent is less than zero for a stable periodic orbit, zero for a quasiperiodic orbit, and greater than zero for a chaotic orbit. Figure 1b shows the maximum Lyapunov exponent as a function of ν, for the bifurcation diagram of Figure 1a, calculated by the Wolf algorithm [*Wolf et al.*, 1985]. It follows from Figure 1 that the global dynamical behavior of nonlinear Alfvén waves contains an admixture of chaotic and ordered regimes, wherein there are periodic windows within a chaotic region and chaotic regions within a periodic window.

[15] An enlargement of a small region of the bifurcation diagram indicated by the arrow in Figure 1a is given in Figure 2a, which displays both attractors (dark) and chaotic saddles (gray) for a period-2 periodic window. This periodic window begins with a saddle-node bifurcation (SNB) at $\nu_{SNB} = 0.07738$, where a pair of period-2 stable (solid line) and unstable (dashed line) periodic orbits are created. The unstable periodic orbit is found by the Newton method [*Curry*, 1979]. The period-2 stable periodic orbit undergoes a cascade of period-doubling bifurcations as ν decreases and turns eventually into a banded chaotic attractor with two bands. This periodic window ends with an interior crisis (IC) at $\nu_{IC} = 0.06212$, when the banded chaotic attractor collides head-on with the period-2 mediating unstable periodic orbit (M) created by the saddle-node bifurcation SNB, which leads to an attractor-widening [*Borotto et al.*, 2004a]. To plot the chaotic saddle, for each value of ν, we plot a straddle trajectory close to the chaotic saddle using the PIM triple algorithm [*Nusse and Yorke*, 1989; *Rempel and Chian*, 2004; *Rempel et al.*, 2004a]. The gray region inside the periodic window in Figure 2a, denotes the surrounding chaotic saddle (SCS) which acts as the transient preceding the convergence of the solutions to a periodic or a chaotic attractor; the surrounding chaotic saddle extends to the chaotic regions outside the periodic window, to the left of IC and to the right of SNB, where it becomes a subset of the chaotic attractor. After crisis, the banded chaotic attractor is converted into a banded chaotic saddle, as shown in Figure 2b. In Figure 2c, we plot the variation of the maximum Lyapunov exponent of the attracting set as a function of ν. Note that the value of the maximum Lyapunov exponent jumps suddenly at IC and SNB, implying an abrupt increase in the degree of chaoticity in nonlinear Alfvén system.

[16] Unstable periodic orbits are the skeleton of a chaotic attractor because chaotic trajectories are closures of the infinite set of unstable periodic orbits [*Ott*, 1993]. In contrast to a periodic attractor thereby all trajectories initiated from any point in the state space are attracted to a stable periodic orbit, in a chaotic attractor all periodic orbits are unstable. Chaotic sets are not necessarily attracting sets. A set of unstable periodic orbits can be chaotic and nonattracting so that the orbits in the neighborhood of this set are eventually repelled from it; nonetheless, this set can contain a chaotic orbit with at least one positive Lyapunov exponent [*Nusse and Yorke*, 1989]. If the chaotic orbit has also one negative Lyapunov exponent the nonattracting set is known as chaotic saddle. Both chaotic saddles and chaotic attractors are composed of unstable periodic orbits. The unstable periodic orbits in a chaotic system have specific functions. For example, we will study the period-2 unstable periodic orbit (M) created at SNB, which is responsible for mediating the onset of an interior crisis at IC which leads to Alfvén crisis-induced intermittency, as well as the laminar phases of Alfvén type-I intermittency. In

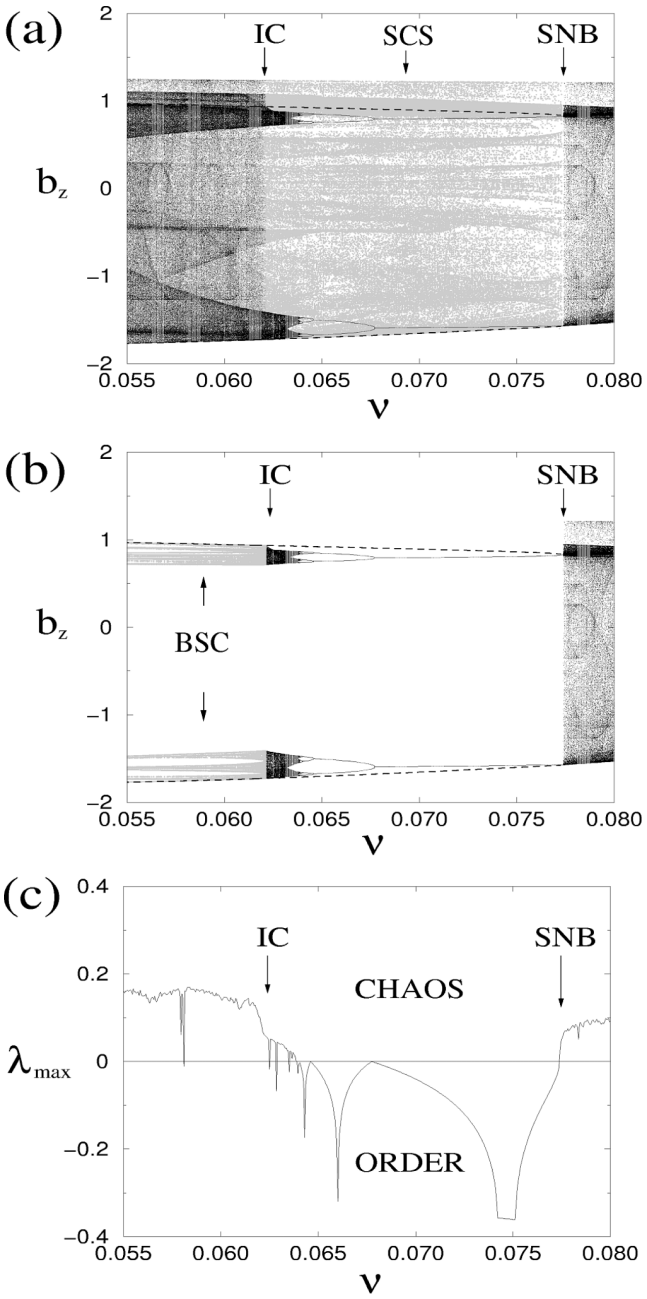

Figure 2. Bifurcation diagram and maximum Lyapunov exponent: period-2 periodic window. (a) Bifurcation diagram, b_z as a function of ν, superimposed by the surrounding chaotic saddle (gray); (b) same as Figure 2a, showing the conversion of the pre-crisis banded chaotic attractor (black) into the post-crisis banded chaotic saddle (gray); (c) maximum Lyapunov exponent, λ_{max} as a function of ν. IC denotes the interior crisis, SNB denotes the saddle-node bifurcation, SCS denotes the surrounding chaotic saddle, BCS denotes the banded chaotic saddle.

addition, we identify a set of coupling unstable periodic orbits (C), located in the gap regions of chaotic saddles embedded in a chaotic attractor, which are responsible for coupling the chaotic saddles resulting in Alfvén crisis-induced intermittency. Examples of mediating and coupling unstable periodic orbits are shown in Figure 3a and Figures 3b–3c, respectively, for $\nu = 0.0616$.

4. Alfvén Type-I Intermittency

[17] As mentioned earlier, a local bifurcation known as saddle-node bifurcation takes place at $\nu_{SNB} = 0.07738$ in Figure 2a, where a pair of period-2 stable and unstable periodic orbits are created. Figure 4a shows a time series of

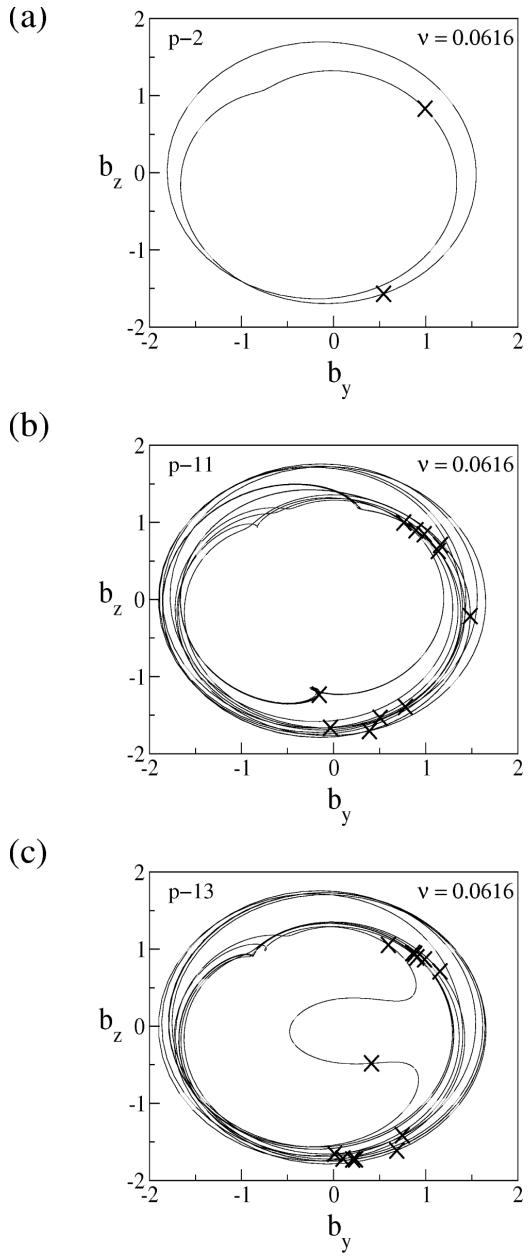

Figure 3. Unstable periodic orbits in the state space and the Poincaré plane for $\nu = 0.0616$. (a) A mediating unstable periodic orbit of period-2 generated via a saddle-node bifurcation at $\nu = 0.07738$, (b) a coupling unstable periodic orbit of period-11 generated via explosion at $\nu = 0.0616$, (c) a coupling unstable periodic orbit of period-13 generated via explosion at $\nu = 0.0621$. Cross denotes the Poincaré points of the unstable periodic orbits.

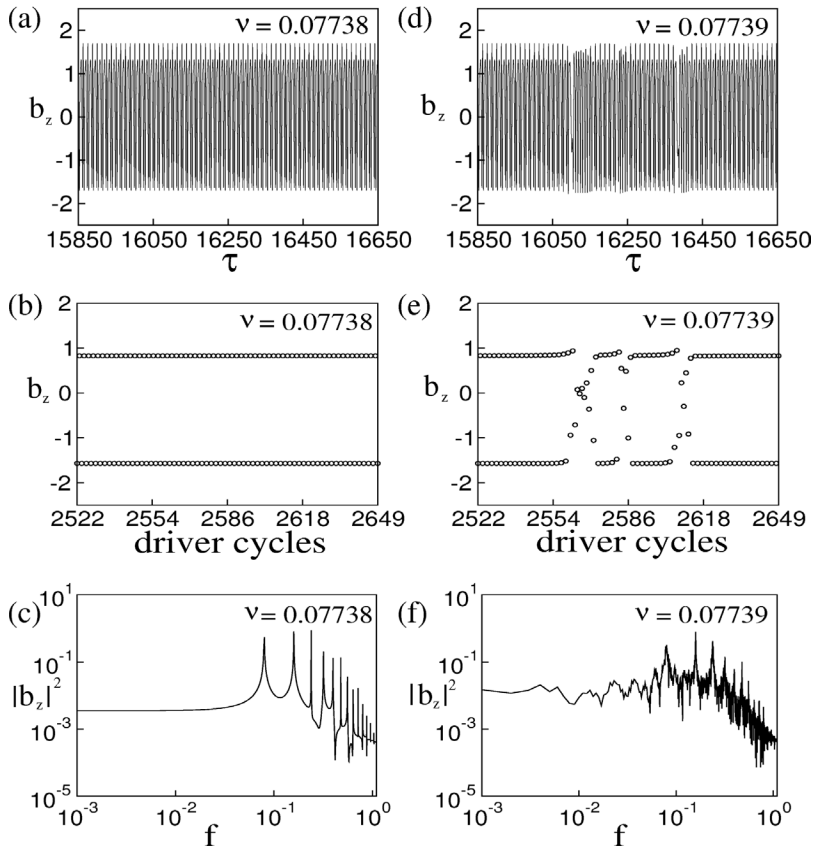

Figure 4. Alfvén type-I intermittency. (a) and (d): Time series b_z as a function of τ for $\nu = 0.07738$ and $\nu = 0.07739$, respectively; (b) and (e): the same time series as Figures 4a and 4d of b_z as a function of the driver cycles; (c) and (f): the power spectrum of Figures 4a and 4d, respectively.

period-2, periodic nonlinear Alfvén wave trains for $\nu = 0.07738$; the same time series as a function of the driver cycles is plotted in Figure 4b; the corresponding power spectrum as a function of wave frequency is given in Figure 4c, which shows discrete peaks typical of a periodic signal. To the right of ν_{SNB}, the system is chaotic, Figure 4d shows a chaotic time series of Alfvén type-I intermittency for $\nu = 0.07739$; the same time series as a function of the driver cycles is given in Figure 4e; the corresponding power spectrum is shown in Figure 4f. The time series of the Alfvén type-I intermittency in Figures 4d–4e demonstrate that the amplitude fluctuations of b_z involves episodic regime switching between periods of laminar fluctuations and periods of bursting fluctuations. In contrast to the discrete power spectrum of the periodic regime seen in Figure 4c, the power spectrum of the chaotic regime before the saddle-node bifurcation is broadband, with a power-law behavior at high frequencies. Note that a typical power density spectrum of interplanetary magnetic field fluctuations show three ranges of frequency with clear power laws: the low-frequency range that belongs to the integral scales, the middle-frequency range that resembles the inertial range predicted by Kolmogorov wherein intermittency is strongly active, and the high-frequency range that represents the dissipation scales [*Bruno et al.*, 2005].

[18] As the Alfvén system undergoes a transition from order to chaos via a saddle-node bifurcation, the surrounding chaotic saddle is converted into a chaotic attractor, as shown in Figure 2a. Figure 5a shows the chaotic attractor (CA) in the Poincaré plane for $\nu = 0.07739$. The surrounding chaotic saddle embedded in the chaotic attractor of Figure 5a is shown in Figure 5b, where we also plotted the locus of the fixed points (cross) of the period-2 unstable periodic orbit (M) just before the transition to chaos, at $\nu_{SNB} = 0.07738$. Unlike M, all the other unstable periodic orbits contained in the surrounding chaotic saddle right after the saddle-node bifurcation (Figure 2a) continue to exist in the chaotic region beyond the saddle-node bifurcation ($\nu > \nu_{SNB}$). Note from Figure 5b that there are gaps in the surrounding chaotic saddle. The conversion from a chaotic saddle to a chaotic attractor, to the right of ν_{SNB}, is due to the creation of new unstable periodic orbits in the gaps regions via the phenomenon of explosion [*Robert et al.*, 2000; *Szábo et al.*, 2000]. An enlargement of the two rectangular regions of Figure 5b is given in Figures 5c and 5d, respectively. Although the period-2 unstable periodic orbit (M) appears only after the saddle-node bifurcation, the system keeps the memory of this orbit before the saddle-node bifurcation. When an unstable periodic orbit, from either the surrounding chaotic saddle or the gap regions in Figure 5b, approaches the vicinities of M, it is decelerated and spends more time in these regions, indicated by Figures 5c–5d. This is due to the synchronization of the unstable periodic orbits of the chaotic attractor with M, which gives rise to the laminar periods of the Alfvén type-I intermittency seen in Figures 4d–4e. When a chaotic orbit

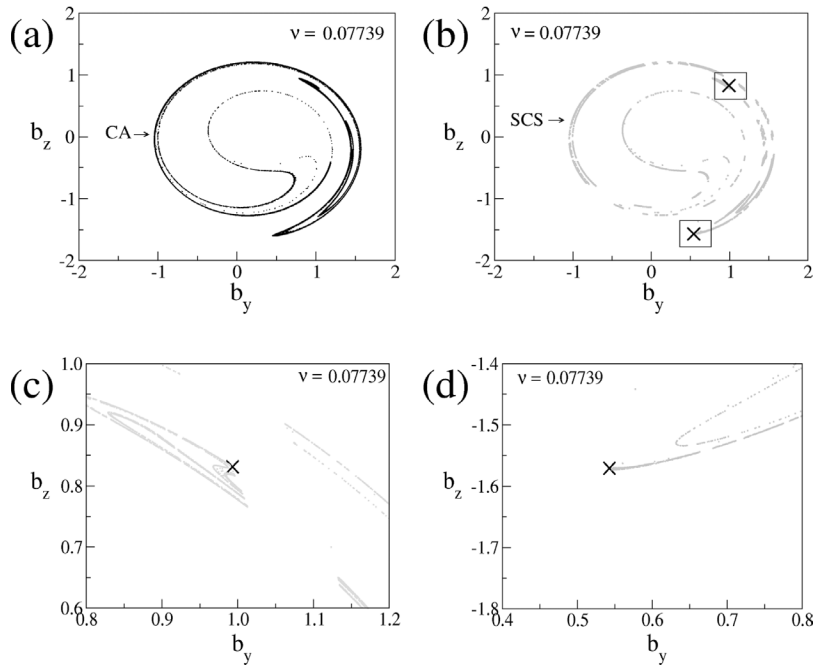

Figure 5. Chaotic attractor and chaotic saddle in Alfvén type-I intermittency for $\nu = 0.07739$. (a) Poincaré map of the chaotic attractor (CA); (b) the surrounding chaotic saddle (SCS, gray) embedded in the chaotic attractor of Figure 5a; (c) and (d) enlargements of the two rectangular regions of (b). Cross denotes the locus of the Poincaré point of the mediating unstable periodic orbit of period-2 created via a saddle-node bifurcation at $\nu_{SNB} = 0.07738$.

moves away from the regions shown in Figures 5c–5d, the orbit becomes desynchronized with respect to M and moves freely along the surrounding chaotic saddle, which then gives rise to the periods of bursting fluctuations seen in Figures 4d–4e.

[19] The average duration of the laminar (quiescent) periods in the time series of the Alfvén type-I intermittency seen in Figures 4d and 4e, known as the characteristic intermittency time, depends on the deviation of the control parameter ν from ν_{SNB}. Close to ν_{SNB} the average time a chaotic orbit spends in the vicinity of the mediating unstable periodic orbit M is very long, and decreases as ν moves away from ν_{SNB}. The characteristic intermittency time τ can be determined by taking the average over a long time series of the time intervals of regime switching from laminar to bursting periods. Figure 6 shows a plot of $\log_{10} \tau$ as a function of $\log_{10} (\nu - \nu_{SNB})$, where the solid line with a slope $\gamma = -0.6$ is a linear fit of the values of the characteristic intermittency time computed from the time series (squares). Figure 6 reveals that the characteristic intermittency time τ decreases with the distance from the critical system parameter ν_{SNB}, following a power-law decay, $\tau \sim (\nu - \nu_{SNB})^{\gamma}$.

5. Alfvén Crisis-Induced Intermittency

[20] A global bifurcation known as interior crisis (IC) takes place at $\nu = 0.06212$, as seen in Figure 2a, which leads to a widening of the chaotic attractor. The occurrence of interior crisis is due to the collision of the banded chaotic attractor with the period-2 mediating unstable periodic orbit (M) created via saddle-node bifurcation at ν_{SNB}. Figure 7a shows the surrounding chaotic saddle SCS (gray), and the banded chaotic attractor CA (black) localized in two separate regions of the phase space, for $\nu = 0.06212$. Figures 7b–7c are enlargements of the two rectangular regions in Figure 7a, respectively, showing the Poincaré points (cross) and its stable manifold SM (light line). The stable manifold of the mediating unstable periodic orbit forms the boundary between the banded and surrounding regions. Figures 7b and 7c reveal that at the onset of crisis

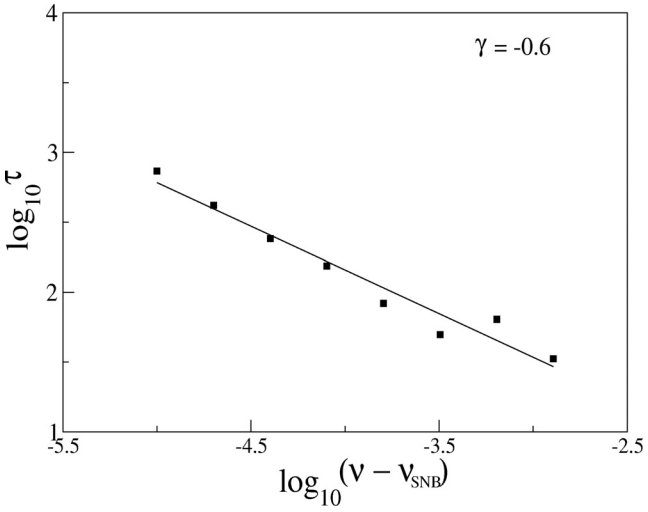

Figure 6. Characteristic intermittency time for Alfvén type-I intermittency. $\log_{10} \tau$ as a function of $\log_{10} (\nu - \nu_{SNB})$.

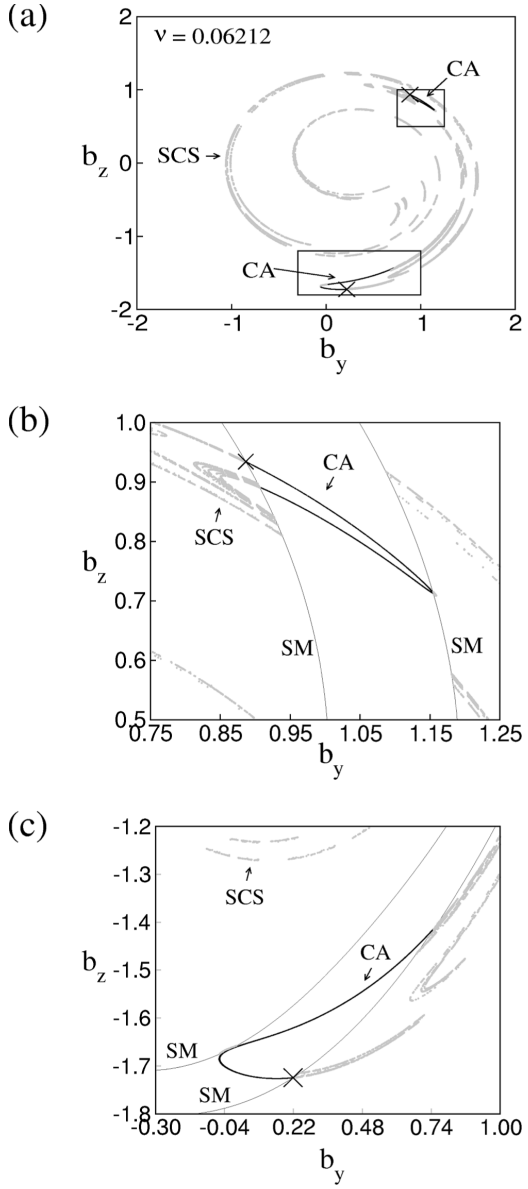

Figure 7. Alfvén interior crisis at $\nu = 0.06212$. (a) Poincaré map of the banded chaotic attractor (CA, black) and the surrounding chaotic saddle (SCS, gray); (b) and (c): enlargements of the two rectangular regions of (a). Cross denotes the Poincaré points of the mediating unstable periodic orbit of period-2 and SM (thin line) denotes its stable manifold.

the chaotic attractor CA collides head on with the mediating unstable periodic orbit and its stable manifold, as well as the surrounding chaotic saddle.

[21] An example of precrisis weakly chaotic time series is given in Figures 8a–8b, and its corresponding power spectrum is given in Figure 8c, for $\nu = 0.06212$. Before crisis, Figures 8a and 8b show that the temporal fluctuations of Alfvén wave amplitude are apparently laminar. The interior crisis leads to a stronger chaos for ν less than ν_{IC}, which induces an intermittent time series exemplified in Figures 8d–8e for $\nu = 0.0616$; the corresponding power spectrum is given in Figure 8f. The Alfvén crisis-induced intermittency in Figures 8a–8b displays random switching between laminar periods and bursting periods of amplitude fluctuations. A comparison of precrisis and postcrisis power spectra of Figures 8c and 8f shows that the discrete spikes are less evident in Figure 8f than Figure 8c, which implies that nonlinear interactions are stronger after crisis.

[22] As the consequence of the chaotic attractor-chaotic saddle collision, after the onset of interior crisis the precrisis banded chaotic attractor turns into a postcrisis strong chaotic attractor, as shown by Figure 9a for $\nu = 0.0616$. Embedded in the strong chaotic attractor are two chaotic saddles (surrounding and banded) and coupling unstable periodic orbits created by explosion after the onset of crisis. Figures 9b shows the numerically found surrounding chaotic saddle (SCS, gray), banded chaotic saddle (BCS, black), and the fixed points of the period-2 mediating unstable periodic orbit (cross). Enlargements of the two rectangular regions of Figure 9b are plotted in Figures 9c and 9d, respectively, where we also show the mediating orbit (cross) and its stable manifold (SM, thin line), which divides the surrounding and banded regions.

[23] Note from Figures 9b to 9d that there are gaps in the surrounding and banded chaotic saddles. These gaps are densely filled by uncountably many coupling unstable periodic orbits (C), created by explosion after the onset of interior crisis [*Robert et al.*, 2000; *Szábo et al.*, 2000], which have components in both surrounding and banded regions and are responsible for the coupling between the two regions. We find numerically two examples of the coupling unstable periodic orbits. Figure 10a shows a coupling unstable periodic orbit of period-11 at $\nu = 0.0616$, which is created via explosion at this value of ν. Enlargements of the two rectangular regions of Figure 10a are given at Figures 10b and 10c, respectively. Figure 11a shows a coupling unstable periodic orbit of period-13 at $\nu = 0.0616$, which is created via explosion at $\nu = 0.0621$. Enlargements of the two rectangular regions of Figure 11a are given in Figures 11b and 11c, respectively. Figures 10 and 11 show that the fixed points of the coupling unstable periodic orbits are located in the gap regions of both surrounding and banded chaotic saddles. The state-space trajectories of the two coupling unstable periodic orbits of Figures 10 and 11 are given in Figures 3b and 3c, respectively.

[24] The average duration of the laminar (quiescent) periods in the time series of the Alfvén crisis-induced intermittency seen in Figures 8d and 8e, i.e., the characteristic intermittency time, depends on the deviation of the control parameter ν from ν_{IC} and decreases as ν moves away from ν_{IC}. The characteristic intermittency time τ can be determined by taking the average over a long time series of the time intervals of regime switching from laminar to bursting periods. Figure 12 shows a plot of $\log_{10} \tau$ as a function of $\log_{10}(\nu_{IC} - \nu)$, where the solid line with a slope $\gamma = -0.78$ is a linear fit of the values of the characteristic intermittency time computed from the time series (squares). Figure 12 reveals that the characteristic intermittency time τ decreases with the distance from the critical system parameter ν_{IC}, following a power-law decay, $\tau \sim (\nu_{IC} - \nu)^{\gamma}$. A comparison of Figures 6 and 12 indicates that the decrease of τ with the deviation from the bifurcation point (ν_{IC}/ν_{SNB})

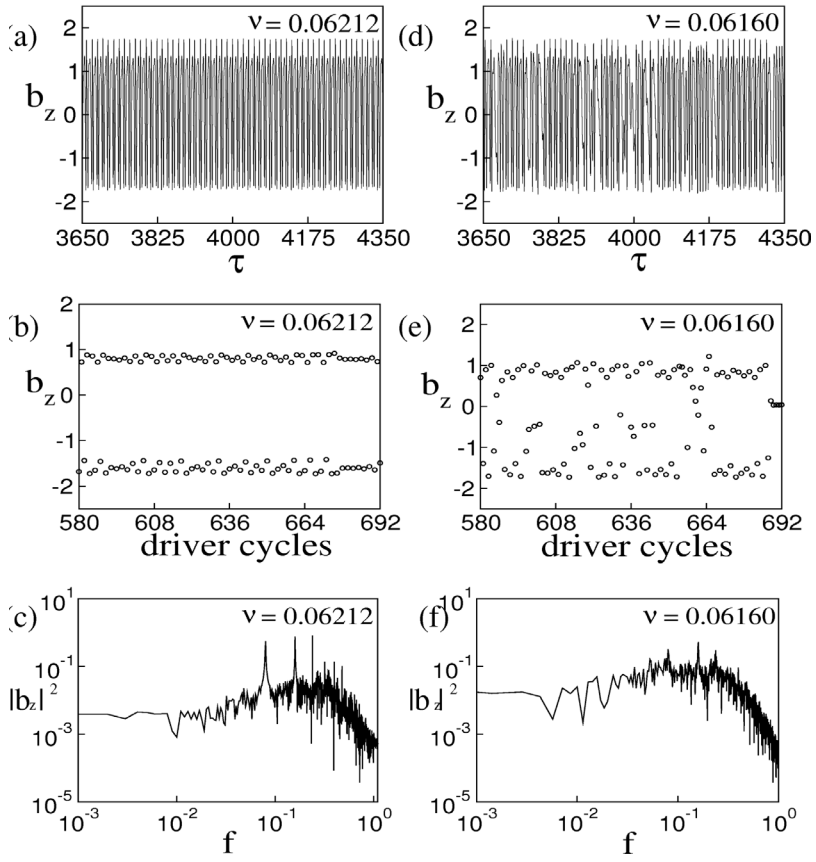

Figure 8. Alfvén crisis-induced intermittency. (a) and (d): Time series b_z as a function of τ for ν = 0.06212 and ν = 0.0616, respectively; (b) and (e): the same time series as Figures 8a and 8d of b_z as a function of the driver cycles; (c) and (f): the power spectrum of Figures 8a and 8d, respectively.

in the Alfvén crisis-induced intermittency is faster than the Alfvén type-I intermittency.

6. Discussion

[25] Large-amplitude interplanetary Alfvén waves can cause intense auroral activities known as HILDCAAs, as a result of the magnetic reconnection between the southward magnetic field components (B_z) of the interplanetary Alfvén waves and the magnetopause magnetic fields, which is responsible for the transfer of solar wind energy to the magnetosphere; during the HILDCAA intervals, there is a close correlation between the minima of B_z and the maxima of the auroral electroject (AE) index [*Tsurutani and Gonzalez*, 1987]. In contrast to solar maximum during which the dominant interplanetary phenomena causing intense geomagnetic storms are the interplanetary manifestation of coronal mass ejections (ICME), during solar minimum the interplanetary Alfvén waves associated with the trailing edge of corotating high-speed streams, are the dominant cause of intermittent magnetic field reconnections in the magnetosphere, intermittent auroral activities, and intermittent injection of plasma sheet energy into the outer regions of the ring current, which are signatures of the HILDCAA events [*Gonzalez et al.*, 1999]. *Tsurutani et al.* [2004] noted that shorter HILDCAA intervals may occur following a geomagnetic storm related to ICME; in particular, they pointed out that although substorms were detected during the HILDCAA intervals, there is little or no relationship between substorm occurrences and AE increases, thus the mechanisms that cause HILDCAAs and substorms may be different. *Diego et al.* [2005] presented evidence of the AE fluctuations directly driven by interplanetary Alfvén waves by examining the AE index variability during 12 passings of corotating fast solar wind streams at the Earth in the ascending phase of solar cycle 23; they applied the Discrete Fourier Transform technique to demonstrate that both the interplanetary Alfvenic magnetic field fluctuations measured by the ACE spacecraft and the AE index have periodicities in the 1 to 10 hour range; in particular, their analysis shows that in all events the magnetic field fluctuations of interplanetary Alfvén waves and the AE index are well correlated. *Tsurutani et al.* [2005] showed that nonlinear Alfvén waves, discontinuities, proton perpendicular acceleration, and magnetic holes/decreases in interplanetary space are interrelated; moreover, interplanetary Alfvén waves are both dispersive and dissipative, indicating that they may be intermediate shocks [*Wu*, 2003]; the turbulence created by the Alfvén wave dissipation is quite complex, containing both propagating (waves) and nonpropagating (mirror mode structures and magnetic decreases) byproducts.

[26] The derivative nonlinear Schrödinger equation (1) which is the basis of our present study contains the effects

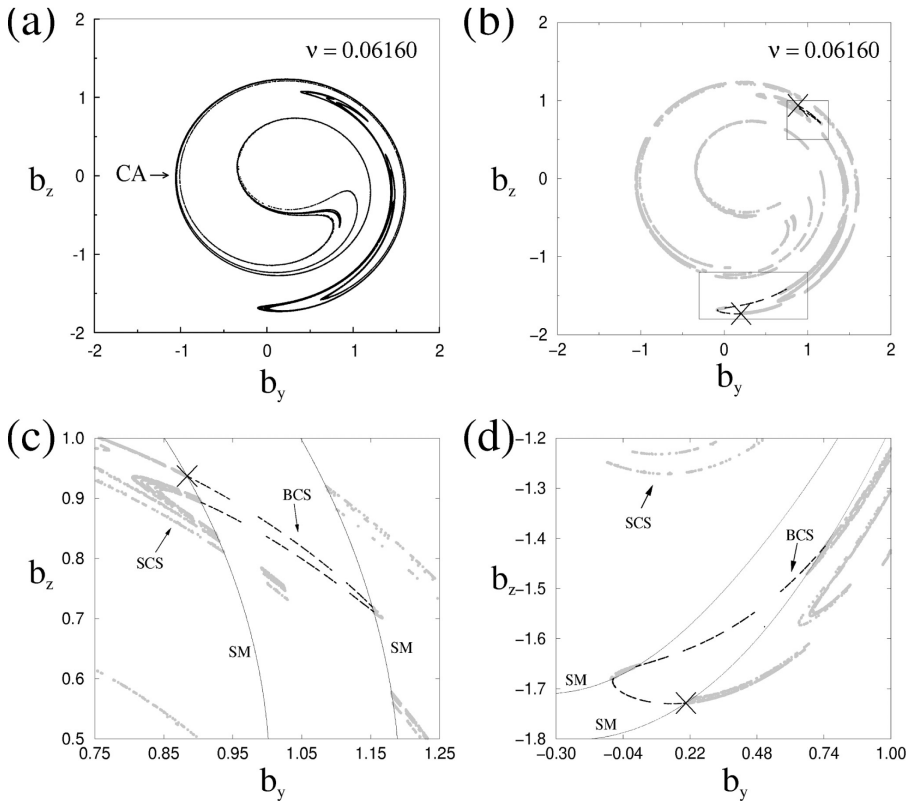

Figure 9. Chaotic attractor and chaotic saddle in Alfvén crisis-induced intermittency for $\nu = 0.0616$. (a) Poincaré map of the chaotic attractor (CA); (b) the surrounding chaotic saddle (SCS, gray) and the banded chaotic saddle (BCS, black) embedded in the chaotic attractor of Figure 9a; (c) and (d): enlargements of the two rectangular regions of (b). Cross denotes the Poincaré points of the mediating unstable periodic orbit of period-2 and SM (thin line) denotes its stable manifold.

of dispersion (μ) and dissipation (η), observed in interplanetary Alfvén waves by *Tsurutani et al.* [2005]. Hence DNLS is a good model for studying the nonlinear evolution of large-amplitude Alfvén waves in the solar wind. The present paper confirmed the previous analysis of *Chian et al.* [1998] and *Borotto et al.* [2001] that DNLS provides important insights for understanding Alfvén intermittency driven by chaos, by showing how intermittent behaviors such as Alfvén type-I intermittency and Alfvén crisis-induced intermittency can arise in plasmas. As pointed out in section 1, a number of papers have characterized interplanetary Alfvén intermittency using the statistical approach [*Marsch and Liu*, 1993; *Marsch and Tu*, 1994; *Sorriso-Valvo et al.*, 1999; *Bruno et al.*, 2001, 2004]. The dynamical systems approach adopted in this paper complements the statistical description of interplanetary Alfvén intermittency. In particular, we succeeded in characterizing the fundamental features of Alfvén intermittency by decomposing an Alfvén chaotic attractor into fundamental unstable structures consisted of chaotic saddles and unstable periodic orbits. This approach enables us to calculate the average duration of the quiescent periods in the Alfvén intermittency, which is related to the dynamical properties of chaotic saddles embedded in the Alfvén chaotic attractor [*Rempel and Chian*, 2005]. Since interplanetary Alfvén waves may be the solar-wind origin of intense geomagnetic activities such as HILDCAAs and given the fact that interplanetary Alfvén waves have been proven to be intermittent by nature, the method introduced in this paper which allows us to predict the average duration of the quiescent periods of interplanetary Alfvén intermittency via numerical simulations can improve the prediction of the abrupt jumps in the Auroral Electroject index, and consequently improve space weather forecasting.

[27] In section 1, we briefly mentioned some works on chaos in solar dynamo, solar corona, and solar wind, putting emphasis on the intermittency in space plasmas. We now discuss in detail the observational and theoretical evidence of the chaotic nature of solar-terrestrial environment. First, let us focus on the Sun and solar wind. A time series analysis of observed solar radio pulsations by *Kurths and Herzel* [1987] suggests that there must be a low-dimensional chaotic attractor. *Mundt et al.* [1991] applied the attractor reconstruction technique to show that the sunspot cycle is chaotic and low-dimensional. *Kurths and Schwarz* [1994] used the method of symbolic dynamics to reveal some order in the fragmentation processes observed in solar radio spikes, and applied the wavelet technique to identify structural differences of the energization processes causing impulsive solar microwave bursts which are a typical transient phenomenon. *Macek and Objska* [1997] invoked the Helios data in low-speed solar streams near the Sun to argue that the inner heliosphere is a low-dimensional chaotic system. *Macek and Radaelli* [2001] obtained evi-

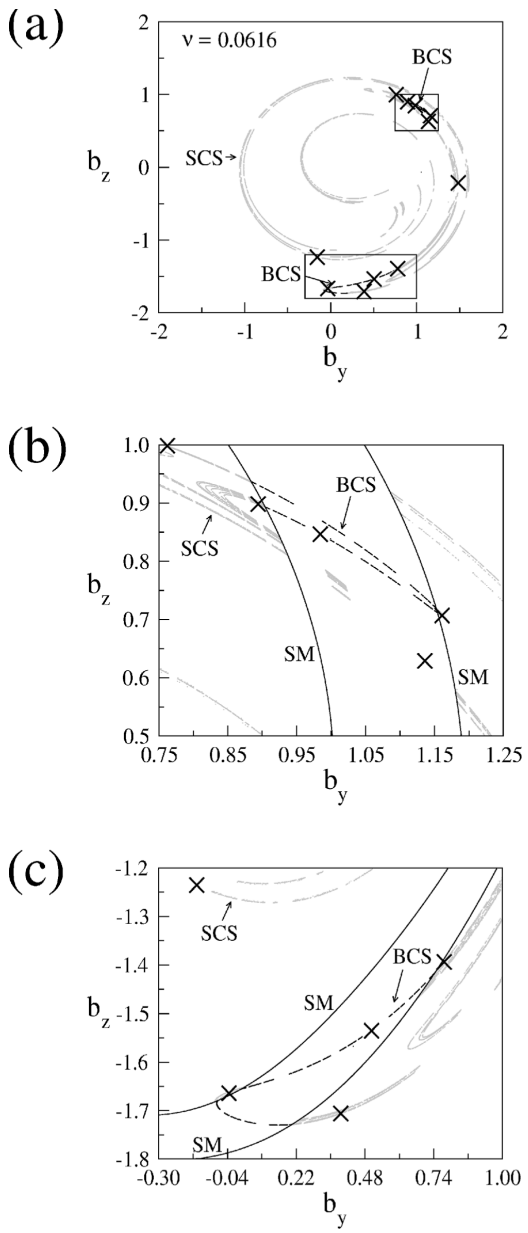

Figure 10. Coupling unstable periodic orbit for Alfvén crisis-induced intermittency at $\nu = 0.0616$. (a) A coupling unstable periodic orbit of period-11 (cross) created via explosion at $\nu = 0.0616$, (b) and (c): enlargements of the two rectangular regions of Figure 10a. The surrounding chaotic saddle (SCS) is indicated by gray, the banded chaotic saddle (BCS) is indicated by black, and SM (thin line) denotes the stable manifold of the mediating unstable periodic orbit of period-2.

dence of chaos in interplanetary Alfvenic fluctuations using the Helios data. *Radaelli and Macek* [2001] showed that the influence of noise in the Helios data can be reduced by a nonlinear filter, which allows them to determine positive values of the largest Lyapunov exponent and the Kolmogorov entropy, indicating chaos in the solar wind flow. *Lei and Meng* [2004] showed that the sunspot cycle is low-dimensional and chaotic by applying the Volterra-Wiener-Korenberg testing method on surrogate data and reconstruction of attractor.

[28] Next, let us turn to magnetosphere. *Baker et al.* [1990] interpreted the evolution from weak to strong geomagnetic activity in terms of deterministic chaos. A correlation dimension analysis of the AE index performed by *Vassiliadis et al.* [1991] showed that the magnetosphere behaves as a low-dimensional chaotic system; their calculation of the Lyapunov exponent of the AL index shows that

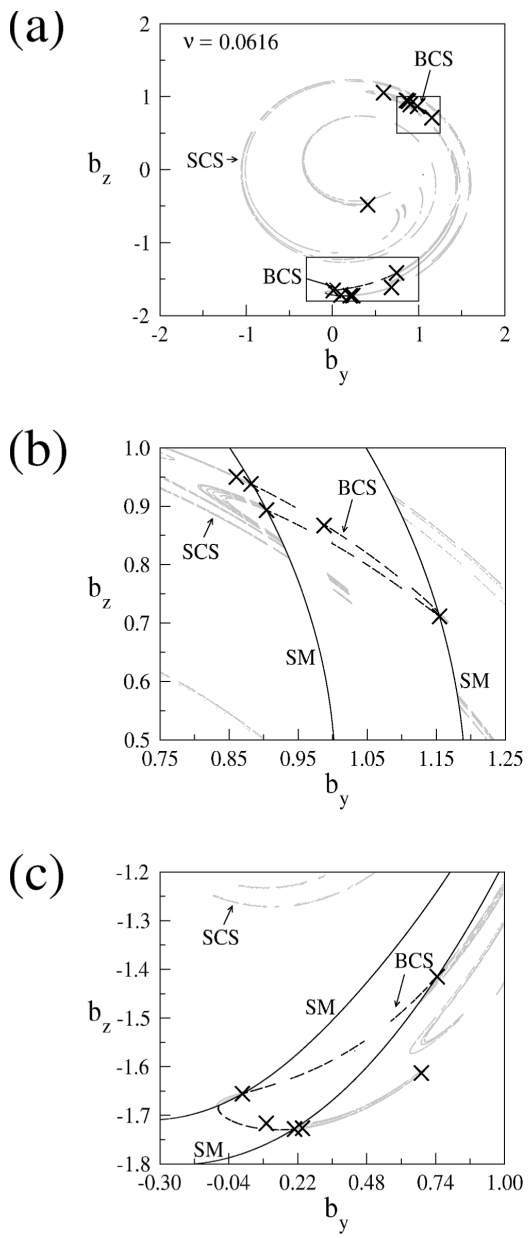

Figure 11. Coupling unstable periodic orbit for Alfvén crisis-induced intermittency at $\nu = 0.0616$. (a) A coupling unstable periodic orbit of period-13 created via explosion at $\nu = 0.0621$; (b) and (c): enlargements of the two rectangular regions of Figure 11a. The surrounding chaotic saddle (SCS) is indicated by gray, the banded chaotic saddle (BCS) is indicated by black, and SM (thin line) denotes the stable manifold of the mediating unstable periodic orbit of period-2.

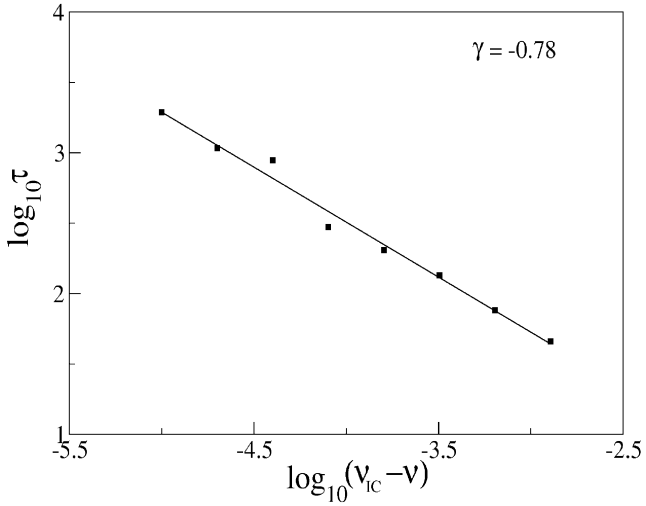

Figure 12. Characteristic intermittency time for Alfvén crisis-induced intermittency. $\log_{10}\tau$ as a function of $\log_{10}(\nu_{IC}-\nu)$.

it is greater than zero which indicates the chaotic behavior of the magnetosphere system. *Klimas et al.* [1992] developed a nonlinear dynamic analog model of magnetotail geomagnetic activity, incorporating both the directly driven and the unloading components of geomagnetic activity, which is capable of exhibiting a transition from regular to chaotic loading and unloading. *Pavlos et al.* [1992] used the estimation of the correlation dimension and the largest Lyapunov exponent to obtain evidence of chaotic attractors for both magnetospheric and solar wind data. *Sharma* [1995] assessed the nonlinear behavior of magnetosphere and analyzed its low dimensionality and predictability. *Klimas et al.* [1996] discussed how to combine a low-dimensional analogue modeling and data-based phase space reconstruction to study the nonlinear dynamical solar wind-magnetosphere coupling. *Pavlos et al.* [1999] carried out a nonlinear analysis of the AE index, obtaining support for chaotic magnetospheric dynamics. *Horton et al.* [1999, 2001] derived a low-dimensional nonlinear dynamical model for the solar wind driven magnetosphere-ionosphere, which exhibits basic properties of a complex dynamical system such as chaos and can be used to predict substorms. *Chian et al.* [2000] and *Chian et al.* [2002c] showed that chaos can appear in a three-wave model of magnetospheric radio emissions involving nonlinear interactions of Langmuir, whistler, and Alfvén waves in the auroral acceleration regions, which can generate type-I intermittency and crisis-induced intermittency in auroral plasmas. *Athanasiu et al.* [2003] obtained evidence of chaos in the time series of energetic magnetospheric ions based on the Lyapunov spectrum, mutual information and prediction models. *Kuo et al.* [2004] studied the chaotic behavior of the trajectories of trapped relativistic electrons interacting with large-amplitude whistler waves in the magnetosphere; a surface of section technique was used to examine the system chaoticity graphically.

[29] Now, let us turn to ionosphere and upper atmosphere. *Huba et al.* [1985] showed that the plasma equations describing the ionospheric turbulence due to interchange instabilities can be reduced to the same set of equations as the Lorenz chaotic attractor [*Lorenz*, 1963]. *Bhattacharyya* [1990] presented observational evidence of the chaotic behavior of ionospheric turbulence from scintillation measurements. *Hall et al.* [1992] identified a chaotic attractor with a fractal dimension around 5 in the in situ rocket measurement of the relative ion density fluctuations of the mesospheric turbulence from 63 km to 72 km altitude. *Kumar et al.* [2004] reported the evidence of low-dimensional chaos in the dynamical behavior of the time series of the fluctuations of the total electron content (TEC) measured in a high-latitude station, using the nonlinear tools of recurrence plots, spatiotemporal entropy, and Lyapunov exponent.

[30] The aforementioned discussions demonstrate that there is a strong interest in the space physics community to explore the chaotic nature of solar-terrestrial environment. Although in this paper we have concentrated on the analysis of Alfvén intermittency driven by chaos, in view of the universal mathematical nature of chaotic systems, the results obtained from our low-dimensional model of Alfvén system can in fact be applied to other nonlinear processes in solar-terrestrial physics. The technique developed in this paper to decompose an Alfvén intermittency in terms of chaotic saddles and unstable periodic orbits can be readily applied to other types of space plasma intermittency driven by chaos.

7. Conclusion

[31] Solar-terrestrial environment is a complex system which exhibits a wealth of nonlinear behaviors. Recent advances in theory, computer modeling, and observation have shed light on the intermittent and chaotic nature of solar-terrestrial environment, from solar interior to solar atmosphere, solar wind, magnetosphere, ionosphere, and atmosphere. Recent advance in dynamical systems research provides powerful nonlinear tools to characterize the fundamental features of intermittency in space plasmas, such as the interplanetary Alfvén intermittency, which elucidates clear links between chaos and intermittency, as seen in this paper.

[32] It is important to point out that the study carried out in this paper was limited to stationary solutions of the derivative nonlinear Schrödinger equation, whereby the dynamical solutions are functions only of the wave phase variable so the solutions are stationary in time. The low-dimensional chaos results obtained in this paper improves our view of the complex nature of space plasmas, e.g., facilitating the numerical determination of the coupling unstable periodic orbits responsible for linking the laminar and bursty phases of Alfvén crisis-induced intermittency, which is difficult to achieve in high-dimensional chaotic systems. It will be highly desirable for future works to extend the present analysis to spatiotemporal solutions of the derivative nonlinear Schrödinger equation and model the dynamical evolution of Alfvén intermittent turbulence both in space and time.

[33] The mathematical model of interplanetary Alfvén intermittency based on the chaos theory is relevant to observation of local dynamics of solar wind as well as global dynamics of intermittency phenomenon in the Earth's magnetosphere shown by geomagnetic indices.

One of the key elements of the space weather forecasting system is the monitoring of local intermittent fluctuations of the magnetic field by spacecrafts located at the L1 point of the solar wind. The information of the local dynamics of solar wind magnetic field is essential to predict the onset and duration of geomagnetic activities due to solar wind driving such as the HILDCAA events [*Tsurutani and Gonzalez*, 1987; *Gonzalez et al.*, 1999; *Tsurutani et al.*, 2004; *Diego et al.*, 2005]. Since the southward turning of solar wind B_z is the cause of magnetic reconnection in the dayside magnetopause, the prediction of the waiting time between the bursts of auroral activities relies on our ability to predict the duration of the laminar period of solar wind B_z. The chaotic model of interplanetary Alfvén intermittency is able to identify the laminar periods of solar wind B_z as shown in Figures 4 and 8 and to provide the scaling laws for the average duration of the laminar periods of solar wind B_z as shown in Figures 6 and 12. This information derived from mathematical modeling can be incorporated into the data assimilation algorithms for space weather forecasting. The auroral electrojet (AE) index, an indicator of the global dynamics of Earth's magnetosphere, is intermittent [*Consolini et al.*, 1996; *Consolini and De Michelis*, 1998, 2005]. The analysis of the HILDCAA events indicates a close correlation between B_z of interplanetary Alfvén waves and the AE index [*Tsurutani and Gonzalez*, 1987; *Diego et al.*, 2005], which suggests that the intermittency in the AE index is related to the intermittency in the solar wind magnetic field. Hence the mathematical model of interplanetary Alfvén intermittency is also relevant for the understanding of the global dynamics of auroral current systems.

[34] The discovery of chaotic attractor in atmosphere by *Lorenz* [1963] has contributed significantly to the improvement of our understanding of the nonlinear dynamics of atmosphere and ocean, leading to a better weather forecasting. Similarly, we expect that the discovery of chaotic saddles in space plasmas can improve our understanding of the nonlinear dynamics of solar-terrestrial environment, which may lead to a better space weather forecasting. Although the presence of chaos in nature renders it impossible to make long-term prediction of weather and space weather, the unstable structures intrinsic in chaotic attractors and chaotic saddles render it possible to make short-term prediction of weather and space weather. The extension of low-dimensional chaos to high-dimensional chaos [*Chian et al.*, 2002b; *Rempel and Chian*, 2003; *Rempel et al.*, 2004b; *Rempel et al.*, 2004c; *Rempel and Chian*, 2005]) will help us to monitor and predict the nonlinear spatiotemporal dynamics and intermittent turbulence in the Earth-ocean-space environment.

[35] **Acknowledgments.** A. C.-L. Chian gratefully acknowledges the award of a visiting professor fellowship by Nagoya University and the kind hospitality of the Solar-Terrestrial Environment Laboratory. This work is supported by CNPq and FAPESP. The authors wish to thank the referees for their valuable comments.

[36] Shadia Rifai Habbal thanks Roberto Bruno and two other referees for their assistance in evaluating this paper.

References

Angelopoulos, V., T. Mukai, and S. Kokubun (1999), Evidence of intermittency in Earth's plasma sheet and implications for self-organized criticality, *Phys. Plasmas*, *6*, 4161.

Athanasiu, M. A., G. P. Pavlos, D. V. Sarafopoulos, and E. T. Sarris (2003), Dynamical characteristics of magnetospheric energetic ion time series: Evidence for low dimensional chaos, *Ann. Geophys.*, *21*, 1995.

Baker, D. N., A. J. Klimas, R. L. McPherron, and J. Buchner (1990), The evolution from weak to strong geomagnetic activity: An interpretation in terms of deterministic chaos, *Geophys. Res. Lett.*, *17*, 41.

Bhattacharyya, A. (1990), Chaotic behavior of ionospheric turbulence from scintillation measurements, *Geophys. Res. Lett.*, *17*, 733.

Boffetta, G., V. Carbone, P. Giuliani, P. Veltri, and A. Vulpiani (1999), Power laws in solar flares: Self-organized criticality or turbulence?, *Phys. Rev. Lett.*, *83*, 4662.

Borotto, F. A., A. C.-L. Chian, A. L. C. Gonzalez, W. D. Gonzalez, and B. T. Tsurutani (2001), Chaotic dynamics of large-amplitude Alfvén-wave trains in the solar wind, *Adv. Space Res.*, *28*, 771.

Borotto, F. A., A. C.-L. Chian, and E. L. Rempel (2004a), Alfvén interior crisis, *Int. J. Bifurcation Chaos*, *14*, 2375.

Borotto, F. A., A. C.-L. Chian, T. Hada, and E. L. Rempel (2004b), Chaos in driven Alfvén systems: Boundary and interior crises, *Physica D*, *194*, 275.

Bruno, R., and V. Carbone (2005), The solar wind as a turbulence laboratory, *Living Rev. Sol. Phys.*, *2*. (Available at http://solarphysics. livingreviews. org.)

Bruno, R., V. Carbone, P. Veltri, E. Pietropaolo, and B. Bavassano (2001), Identifying intermittency events in the solar wind, *Planet. Space Sci.*, *49*, 1201.

Bruno, R., L. Sorriso-Valvo, V. Carbone, and B. Bavassano (2004), A possible truncated-Levy-flight statistics recovered from interplanetary solar-wind velocity and magnetic-field fluctuations, *Europhys. Lett*, *66*, 146.

Bruno, R., V. Carbone, B. Bavassano, and L. Sorriso-Valvo (2005), Observations of magnetodydrodynamic turbulence in the 3D heliosphere, *Adv. Space Res.*, *35*, 939.

Burlaga, L. F. (1988), Period doubling in the outer heliosphere, *J. Geophys. Res.*, *93*, 4103.

Burlaga, L. F. (1991), Multifractal structure of speed fluctuations in recurrent streams at 1-AU and 6-AU, *Geophys. Res. Lett.*, *18*, 1651.

Burlaga, L. F., and A. F. Viñas (2004), Multiscale structure of the magnetic field and speed at 1 AU during the declining phase of solar cycle 23 described by a generalized Tsallis probability distribution function, *J. Geophys. Res.*, *109*, A12107, doi:10.1029/2004JA010763.

Buti, B. (1992), Chaotic Alfvén waves in multispecies plasmas, *J. Geophys. Res.*, *97*, 4229.

Buti, B. (1997), Control of chaos in dusty plasmas, *Phys. Lett. A*, *235*, 241.

Buti, B. (1999), Chaos in magnetoplasmas, *Nonlinear Procr. Geophys.*, *6*, 129.

Buti, B., V. L. Galinski, V. I. Shevchenko, G. S. Lakhina, B. T. Tsurutani, B. E. Goldstein, P. Diamond, and M. V. Medvedev (1999), Evolution of nonlinear Alfvén waves in streaming inhomogeneous plasmas, *Astrophys. J.*, *523*, 849.

Chang, T., S. W. Y. Tam, C. C. Wu, and G. Consolini (2003), Complexity, forced and/or self-organized criticality, and topological phase transitions in space plasmas, *Space Sci. Rev.*, *107*, 425.

Chang, T., S. W. Y. Tam, and C. C. Wu (2004), Complexity induced anisotropic bimodal intermittent turbulence in space plasmas, *Phys. Plasmas*, *11*, 1287.

Charbonneau, P., G. Balis-Laurier, and C. St-Jean (2004), Intermittency and phase persistence in a Babcock-Leighton model of the solar cycle, *Astrophys. J.*, *616*, L183.

Charbonneau, P., C. St-Jean, and P. Zacharias (2005), Fluctuations in Babcock-Leighton dynamos. I. Period doubling and transition to chaos, *Astrophys. J.*, *619*, 613.

Chian, A. C.-L., F. A. Borotto, and W. D. Gonzalez (1998), Alfvén intermittent turbulence driven by temporal chaos, *Astrophys. J.*, *505*, 993.

Chian, A. C.-L., F. A. Borotto, S. R. Lopes, and J. R. Abalde (2000), Chaotic dynamics of nonthermal planetary radio emission, *Planet. Space Sci.*, *48*, 9.

Chian, A. C.-L., F. A. Borotto, and E. L. Rempel (2002a), Alfvén boundary crisis, *Int. J. Bifurcation Chaos*, *12*, 1653.

Chian, A. C.-L., E. L. Rempel, E. E. Macau, R. R. Rosa, and F. Christiansen (2002b), High-dimensional interior crisis in the Kuramoto-Sivashinsky equation, *Phys. Rev. E*, *65*, 035203(R).

Chian, A.C.-L., E. L. Rempel, and F. A. Borotto (2002c), Chaos in magnetospheric radio emissions, *Nonlinear Proc. Geophys.*, *9*, 435.

Choe, W., H. J. Kim, G. Rostoker, and Y. Kamide (2002), Nonlinear time series analysis of interpeak intervals of AL data, *J. Geophys. Res.*, *107*(A11), 1392, doi:10.1029/2001JA002010.

Consolini, G., and P. De Michelis (1998), Non-Gaussian distribution function of AE-index fluctuations: Evidence for time intermittency, *Geophys. Res. Lett.*, *25*, 4087.

Consolini, G., and P. De Michelis (2002), Fractal time statistics of AE-index burst waiting times: Evidence of metastability, *Nonlinear Proc. Geophys.*, *9*, 419.

Consolini, G., and P. De Michelis (2005), Local intermittency measure analysis of AE index: The directly driven and unloading component, *Geophys. Res. Lett.*, *32*, L05101, doi:10.1029/2004GL022063.

Consolini, G., M. F. Marcucci, and H. Candidi (1996), Multifractal structure of auroral electroject index data, *Phys. Rev. Lett.*, *76*, 4082.

Curry, J. H. (1979), An algorithm for finding closed orbits, in *Global Theory of Dynamical Systems*, edited by Z. Citecki and C. Robinson, p. 111, Springer, New York.

De Oliveira, L. P. L., F. B. Rizzato, and A. C.-L. Chian (1997), Intrinsic modulational Alfvénic turbulence, *J. Plasma Phys.*, *58*, 441.

Diego, P., M. Storini, M. Parisi, and E. G. Cordaro (2005), AE index variability during corotating fast solar wind streams, *J. Geophys. Res.*, *110*, A06105, doi:10.1029/2004JA010715.

Dmitruk, P., D. O. Gómez, and E. E. de Luca (1998), Magnetohydrodynamic turbulence of coronal active regions and the distribution of nanoflares, *Astrophys. J.*, *505*, 974.

Georgoulis, M. K., M. Velli, and G. Einaudi (1998), Statistical properties of magnetic activity in the solar corona, *Astrophys. J.*, *497*, 957.

Ghosh, S., and K. Papadopoulos (1987), The onset of Alfvénic turbulence, *Phys. Fluids*, *30*, 1371.

Gómez, D. O., P. D. Mininni, and P. Dmitruk (2004), Direct numerical simulatieons of helical dynamo action: MHD and beyond, *Nonlinear Proc. Geophys.*, *11*, 619.

Gonzalez, W. D., B. T. Tsurutani, and A. L. C. de Gonzalez (1999), Interplanetary origin of geomagnetic storms, *Space Sci. Rev.*, *88*, 529.

Gulamali, M. Y., and P. J. Cargill (2001), Ulysses observations of magnetohydrodynamic turbulence in corotating interaction regions, *J. Geophys. Res.*, *106*, 15,687.

Hada, T., C. F. Kennel, B. Buti, and E. Mjolhus (1990), Chaos in driven Alfvén systems, *Phys. Fluids B*, *2*, 2581.

Hall, C., T. A. Blix, and E. V. Thrane (1992), Attractor dimensionality for mesospheric turbulence, *J. Geophys. Res.*, *97*, 153.

Hnat, B., S. C. Chapman, G. Rowlands, N. W. Watkins, and M. P. Freeman (2003), Scaling in long term data sets of geomagnetic indices and solar wind epsilon as seen by WIND spacecraft, *Geophys. Res. Lett.*, *30*(22), 2174, doi:10.1029/2003GL018209.

Hnat, B., S. C. Chapman, and G. Rowlands (2005), Compressibility in solar wind plasma turbulence, *Phys. Rev. Lett.*, *94*, 204502.

Horton, W., J. P. Smith, R. Weigel, C. Crabtree, I. Doxas, B. Goode, and J. Cary (1999), The solar-wind driven magnetosphere-ionosphere as a complex dynamical system, *Phys. Plasmas*, *6*, 4178.

Horton, W., R. S. Weigel, and J. C. Sprott (2001), Chaos and the limits of predictability for the solar-wind-driven magnetosphere-ionosphere system, *Phys. Plasmas*, *8*, 2946.

Hoyng, P. (1993), Helicity fluctuations in mean-field theory: An explanation for the variability of the solar-cycle, *Astron. Astrophys.*, *272*, 321.

Huba, J. D., A. B. Hassam, I. B. Schwartz, and M. J. Keskinen (1985), Ionospheric turbulence: Interchange instabilities and chaotic fluid behavior, *Geophys. Res. Lett.*, *12*, 65.

Kamide, Y., and S. Kokubun (1996), Two-component auroral electrojet: Importance for substorm studies, *J. Geophys. Res.*, *101*, 13,027.

Klimas, A. J., D. N. Baker, D. A. Roberts, D. H. Fairfield, and J. Buchner (1992), A nonlinear dynamic analog model of geomagnetic activity, *J. Geophys. Res.*, *97*, 12,253.

Klimas, A. J., D. Vassiliadis, D. N. Baker, and D. A. Roberts (1996), The organized nonlinear dynamics of the magnetosphere, *J. Geophys. Res.*, *101*, 13,089.

Kovács, P., V. Carbone, and Z. Vörös (2001), Wavelet-based filtering of intermittent events from geomagnetic time-series, *Planet. Space. Sci.*, *49*, 1219.

Kremliosvsky, M. N. (1995), Limits of predictability of solar-activity, *Solar Phys.*, *159*, 371.

Krishan, V., and L. Nocera (2003), Relaxed states of Alfvénic turbulence, *Phys. Lett. A*, *315*, 389.

Kumar, K. S., C. V. A. Kumar, B. George, G. Renuka, and C. Venugopal (2004), Analysis of the fluctuations of the total electron content (TEC) measured at Goose Bay using tools of nonlinear methods, *J. Geophys. Res.*, *109*, A02308, doi:10.1029/2002JA009768.

Kuo, S. P., P. Kossey, J. T. Huynh, and S. S. Kuo (2004), Amplification of whistler waves for the precipitation of trapped relativistic electrons in the magnetosphere, *IEEE Trans. Plasma Sci.*, *32*, 362.

Kurths, J., and H. Herzel (1987), An attractor in a solar time-series, *Physica D*, *25*, 165.

Kurths, J., and U. Schwarz (1994), Chaos theory and radio-emission, *Space Sci. Rev.*, *68*, 171.

Kurths, J., A. Brandenburg, U. Feudel, and W. Jensen (1993), Chaos in nonlinear dynamo models, *IAU Symp.*, *157*, 83.

Lei, M., and G. Meng (2004), Detecting nonlinearity of sunspot number, *Int. J. Nonlinear Sci. Numer. Sim.*, *5*, 321.

Leubner, M. P., and Z. Voros (2005), A nonextensive entropy approach to solar wind intermittency, *Astrophys. J.*, *618*, 547.

Lorenz, E. N. (1963), Deterministic non-periodic flow, *J. Atmos. Sci.*, *20*, 130.

Macek, W. M., and L. Objska (1997), Fractal analysis of the solar wind flow in the inner heliosphere, *Chaos Solitions Fractals*, *8*, 1601.

Macek, W. M., and S. Radaelli (2001), Testing for chaos in the solar wind and Alfvénic fluctuations, *Adv. Space Res.*, *28*, 775.

Markovskii, S. A., and J. V. Hollweg (2004), Intermittent heating of the solar corona by heat flux-generated ion cyclotron waves, *Astrophys. J.*, *609*, 1112.

Marsch, E., and S. Liu (1993), Structure functions and intermittency of velocity fluctuations in the inner solar-wind, *Ann. Geophys.*, *11*, 227.

Marsch, E., and C. Y. Tu (1994), Non-Gaussian probability-distribution of solar-wind fluctuations, *Ann. Geophys.*, *12*, 1127.

Matthaeus, W. H., G. P. Zank, C. W. Smith, and S. Oughton (1999), Turbulence, spacial transport, and heating of the solar wind, *Phys. Rev. Lett.*, *82*, 3444.

Moussas, X., J. M. Polygiannakis, P. Preka-Papadema, and G. Exarhos (2005), Solar cycles: A tutorial, *Adv. Space Res.*, *35*, 725.

Mundt, M. D., W. B. Maguire, and R. R. P. Chase (1991), Chaos in the sunspot cycle - analysis and prediction, *J. Geophys. Res.*, *96*, 1705.

Nocera, L., and B. Buti (1996), Acceleration of Alfvén solitons, *Phys. Scr. T*, *63*, 186.

Nusse, H. E., and J. A. Yorke (1989), A procedure for finding numerical trajectories on chaotic saddles, *Physica D*, *36*, 137.

Ossendrijver, M., and E. Covas (2003), Crisis-induced intermittency due to attractor-widening in a buoyancy-driven solar dynamo, *Int. J. Bifurcation Chaos*, *13*, 2327.

Ott, E. (1993), *Chaos in Dynamical Systems*, Cambridge Univ. Press, New York.

Padhye, N. S., S. W. Smith, and W. H. Matthaeus (2001), Distribution of magnetic field components in the solar wind plasma, *J. Geophys. Res.*, *106*, 18,635.

Pagel, C., and A. Balogh (2003), Radial dependence of intermittency in the fast polar solar wind magnetic field using Ulysses, *J. Geophys. Res.*, *108*(A1), 1012, doi:10.1029/2002JA009498.

Patourakos, S., and J. C. Vial (2002), Intermittent behavior in the transition region and the low corona of the quiet Sun, *Astron. Astrophys.*, *385*, 1073.

Pavlos, G. P., G. A. Kyriakou, A. G. Rigas, P. I. Liatsis, P. C. Trochoutsos, and A. A. Tsonis (1992), Evidence for strange attractor structures in space plasmas, *Ann. Geophys.*, *10*, 309.

Pavlos, G. P., D. Kugiumtyis, M. A. Athanasiu, N. Hatzigeorgiu, D. Diamantidis, and E. T. Sarris (1999), Nonlinear analysis of magnetospheric data. part II. Dynamical characteristics of the AE index time series and comparison with nonlinear surrogate data, *Nonlinear Proc. Geophys.*, *6*, 79.

Price, C. P., and D. Prichard (1993), The nonlinear response of the magnetosphere, *Geophys. Res. Lett.*, *20*, 771.

Pu, Z. Y., and X. M. Wang (1997), Structure instability and nonlinear evolution of magnetic islands at the magnetopause, *J. Geophys. Res.*, *102*, 6.

Radaelli, S., and W. M. Macek (2001), Lyapunov exponent and entropy of the solar wind flow, *Planet. Space Sci.*, *49*, 1211.

Rempel, E. L., and A. C.-L. Chian (2003), High-dimensional chaotic saddles in the Kuramoto-Sivashinsky equation, *Phys. Lett. A*, *319*, 104.

Rempel, E. L., and A. C.-L. Chian (2004), Alfvén chaotic saddles, *Int. J. Bifurcation Chaos*, *14*, 4009.

Rempel, E. L., and A. C.-L. Chian (2005), Intermittency induced by attractor-merging crisis in Kuramoto-Sivashinsky equation, *Phys. Rev. E*, *71*, 061203.

Rempel, E. L., A. C.-L. Chian, E. E. N. Macau, and R. R. Rosa (2004a), Analysis of chaotic saddles in low-dimensional dynamical systems: The derivative nonlinear Schrödinger equation, *Physica D*, *199*, 407.

Rempel, E. L., A. C.-L. Chian, E. E. Macau, and R. R. Rosa (2004b), Analysis of chaotic saddles in high-dimensional dynamical systems: The Kuramoto-Sivashinsky equation, *Chaos*, *14*, 545.

Rempel, E. L., A. C-L. Chian, A. J. Preto, and S. Stephany (2004c), Intermittent chaos driven by nonlinear Alfvén waves, *Nonlinear Proc. Geophys.*, *11*, 691.

Robert, C., K. T. Alligood, E. Ott, and J. A. Yorke (2000), Explosions of chaotic sets, *Physica D*, *144*, 44.

Sharma, A. S. (1995), Assessing the magnetospheres nonlinear behavior - its dimension is low, its predictability high, *Rev. Geophys.*, *33*, 645.

Sorriso-Valvo, L., V. Carbone, P. Veltri, G. Consolini, and R. Bruno (1999), Intermittency in the solar wind turbulence through probability distribution functions of fluctuations, *Geophys. Res. Lett.*, *26*, 1801.

Stepanova, M. V., E. E. Antonova, and O. Troshichev (2003), Intermittency of magnetospheric dynamics through non-Gaussian distribution function of PC-index fluctuations, *Geophys. Res. Lett.*, *30*(3), 1127, doi:10.1029/2002GL016070.

Szabó, K. G., Y.-C. Lai, T. Tel, and C. Grebogi (2000), Topological gap filling at crisis, *Phys. Rev. E*, *61*, 5019.

Tobias, S. M., N. O. Weiss, and V. Kirk (1995), Chaotically modulated stellar dynamos, *Mon. Not. R. Astron. Soc.*, *273*, 1150.

Tsurutani, B. T., and W. D. Gonzalez (1987), The cause of high-intensity long-duration continuous AE activity (HILDCAAS): Interplanetary Alfvén wave trains, *Planet. Space Sci.*, *35*, 405.

Tsurutani, B. T., W. D. Gonzalez, F. Guarnieri, Y. Kamide, X. Y. Zhou, and J. K. Arballo (2004), Are high-intensity long-duration continuous AE activity (HILDCAA) events substorm expansion events?, *J. Atmos. Sol. Terr. Phys.*, *66*, 167.

Tsurutani, B. T., G. S. Lahkina, J. S. Pickett, F. L. Guanieri, N. Lin, and B. E. Goldstein (2005), Nonlinear Alvén waves, discontinuities, proton perpendicular acceleration, and magnetic holes/decreases in interplanetary space and the magnetosphere: Intermediate shocks?, *Nonlinear Proc. Geophys.*, *12*, 321.

Vassiliadis, D., A. S. Sharma, and K. Papadopoulos (1991), Lyapunov exponent of magnetospheric activity from AL time-series, *Geophys. Res. Lett*, *18*, 1643.

Veltri, P., G. Nigro, F. Malara, V. Carbone, and A. Mangeney (2005), Intermittency in MHD turbulence and coronal nanoflares modeling, *Nonlinear Proc. Geophys.*, *12*, 245.

Vörös, Z., et al. (2004), Magnetic turbulence in the plasma sheet, *J. Geophys. Res.*, *109*, A11215, doi:10.1029/2004JA010404.

Weiss, N. O., and S. M. Tobias (2000), Physical causes of solar activity, *Space Sci. Rev.*, *94*, 99.

Weygand, J. M., et al. (2005), Plasma sheet turbulence observed by Cluster II, *J. Geophys. Res.*, *110*, A01205, doi:10.1029/2004JA010581.

White, R., L. Chen, and Z. H. Lin (2002), Resonant plasma heating below the cyclotron frequency, *Phys. Plasmas*, *9*, 1890.

Wolf, A., J. B. Swift, H. L. Swinney, and J. A. Vastano (1985), Determining Lyapunov exponents from a time series, *Physica D*, *16*, 285.

Wu, C. C. (2003), MKDVB and CKB shock waves, *Space Sci. Rev.*, *107*, 403.

Zelenyi, L. M., and A. V. Milovanov (2004), Fractal topology and strange kinetics: From percolation theory to problems in cosmic electrodynamics, *Phys. Uspekhi*, *47*, 749.

A. C.-L. Chian and W. M. Santana, National Institute for Space Research (INPE) and World Institute for Space Environment Research (WISER), P. O. Box 515, São José dos Campos, São Paulo 12227-010, Brazil. (achian@dge.inpe.br; wanderson@dge.inpe.br)

Y. Kamide, Nagoya University, Solar-Terrestrial Environment Laboratory, Toyokawa 4428507, Japan. (kamide@stelab.nagoya-u.ac.jp)

E. L. Rempel, Institute of Aeronautical Technology (ITA) and World Institute for Space Environment Research (WISER), São José dos Campos, São Paulo 12228-900, Brazil. (rempel@ita.br)